LA-UR- 00-1293

Approved for public release; distribution is unlimited.

Title: Simulation of an Acoustic Helmholtz Resonator Using Computational Fluid Dynamics

Author(s): M.J. Broxton, C.N. Ammerman, R.A. Martin
Engineering Sciences and Applications Division
Design Engineering Group

S. Backhaus
Material Science Technology Division
Condensed Matter and Thermal Physics Group

Submitted to: ASME 2000 Fluids Engineering Division Summer Meeting
June 11-15, 2000, Boston, Massachusetts

Los Alamos
NATIONAL LABORATORY

DISCLAIMER

Proceedings of ASME FEDSM'00
ASME 2000 Fluids Engineering Division Summer Meeting
June 11-15, 2000, Boston, Massachusetts

FEDSM2000-11295

SIMULATION OF AN ACOUSTIC HELMHOLTZ RESONATOR USING COMPUTATIONAL FLUID DYNAMICS

M.J. Broxton[1], S. Backhaus[2], C.N. Ammerman[1], and R.A. Martin[1]
[1]Engineering Sciences and Applications Division, Design Engineering Group
[2]Material Science and Technology Division, Condensed Matter and Thermal Physics Group
Los Alamos National Laboratory
Los Alamos, New Mexico 87545

ABSTRACT

This paper summarizes the results of a computer simulation of an acoustic Helmholtz resonator and comparison of those results with experimental data. A commercial CFD code has been used to model, solve, and analyze the simulation. The goal of these efforts is to provide an inexpensive and reliable method for studying oscillating-flow minor losses affecting the performance of thermoacoustic engines. Although there are extensive catalogs of minor losses in steady flow, very little work has been done in oscillatory flow. Researchers at Los Alamos National Laboratory have constructed an acoustic Helmholtz resonator that will allow them to observe oscillating-flow losses of common pipe fittings including straight pipes, elbows, diffusers, and t-junctions. The computer model discussed in this paper is designed to closely mirror the experiment being run in the laboratory. By combining the results of the experiment with those of the computer model, scientists hope to learn how to further reduce operating losses of thermoacoustic engines or other oscillating-flow machines.

INTRODUCTION

The Carnot efficiency has long been the goal in heat engine design. Unfortunately, this theoretical maximum efficiency is far from the grasp of any currently developed heat engine, but researchers go to great lengths to coax another one or two percent of efficiency from their designs. These small but significant improvements can be made by carefully analyzing elements such as the engine's component geometry. This effort focuses on studying minor losses in an exciting new contender in the heat engine arena: the thermoacoustic-Stirling engine.

As the name suggests, the thermoacoustic-Stirling engine generates acoustic power, which is transmitted without the aid of moving parts. The realization of a no-moving-parts heat engine is a very strong advantage of using acoustic power. The thermoacoustic-Stirling engine also promises to be very efficient. The rough prototypes developed in labs already demonstrate an efficiency of 0.30, or 41% of the Carnot efficiency. This is already comparable to the gasoline combustion engine and piston-driven Stirling engines [1].

This paper summarizes the results of a computer model of an acoustic resonator. The acoustic resonator is an apparatus created to observe oscillating fluid flow through impediments common to pipe geometries including straight pipes, elbows, diffusers, and t-junctions. AEA Technologies' computational fluid dynamics code CFX 4.2 has been used to model, solve, and analyze the simulation. The ultimate goal of these efforts is to provide an inexpensive and reliable method for analyzing the effectiveness of different pipe geometries and to provide data that can improve the efficiency of thermoacoustic engines.

NOMENCLATURE

A	amplitude of oscillation
E	energy stored in oscillation (W)
T	period of oscillation (s)
t	time (s)
α	constant related to resonator geometry
β	constant related to minor losses

METHODS AND THEORY

Thermoacoustics

A thermoacoustic-Stirling heat engine (TASHE) is a device that absorbs heat from a high temperature source, rejects some of that heat at a low temperature sink [1], and in the process produces acoustic power. The acoustic power is in the form of pressure and velocity oscillations of the engine's working fluid, typically high-pressure helium. The engine uses the Stirling heat engine cycle to perform the three functions listed above. The use of the Stirling cycle in acoustic engines has increased their efficiency by approximately 50% over the previously used standing-wave cycle. Use of the Stirling cycle, however, requires some complicated duct-work that may lead to energy dissipation due to minor losses.

To force the working fluid through the Stirling cycle, an acoustic traveling wave is propagated through a regenerative heat exchanger (regenerator) sandwiched between high- and low-temperature heat exchangers. A traveling wave has pressure and velocity oscillations in time phase. Standing waves, not traveling waves, naturally occur in the geometry of an acoustic engine that usually contains a resonator to set the operating frequency. The TASHE then must convert the resonator's standing waves to traveling waves in the vicinity of the regenerator. To accomplish this, the engine uses a carefully designed acoustic network. This network usually contains expansions, diffusers, pipe bends, etc. which are potential sources of minor losses due to flow separation and secondary flows.

Backhaus and Swift [1] hope to make improvements to the efficiency of the engine through a characterization of high Reynolds number, oscillating fluid flow in the acoustic network components. They have created an experiment that will allow them to make simple measurements of these characteristics in various pipe geometries. Their experiment, an acoustic resonator, allows simple oscillations of a gas to be studied. The geometry of the acoustic resonator is shown in Fig. 1. The overall length of this resonator is approximately 1.4 m. The connecting pipe is 0.0254 m in diameter. Tapered transition sections connect the pipe with the bulbs. These sections have a 7° taper. The bulb on the right is filled with a working fluid (in this case, argon gas) at high pressure. At the beginning of an experiment, the valve is opened allowing the high-pressure gas to expand into the low-pressure section on the left. An oscillatory flow then develops. Since no external power source is driving the oscillations, the losses gradually reduce the oscillating amplitude to zero. Pressure is measured in each of the bulbs as a function of time to study the effects of losses. The resonator is designed such that simple pipe fittings, such as a 90° elbow, can be inserted and the additional losses due to the fitting determined.

The computer model discussed in this paper is designed to closely mirror the experiment being run in the laboratory. Based on the results of this experiment and the computer model, the scientists hope to learn how to improve the structure of the engine. The first test of the resonator is designed to determine the losses due to the basic configuration of the resonator, without any fittings. By incorporating the results of this and several other efficiency-enhancement studies, Backhaus and Swift hope to bring thermoacoustic devices into competition with other modern heat engines.

Computational Model

A 2-D CFD model was constructed to complement the laboratory experiment. The CFD model has been generated and solved using the CFX4.2 commercial code developed by AEA Technology. CFX4.2 is extremely flexible allowing for a wide range of possible fluid dynamics scenarios. The CFX package is a suite of three basic programs that allow modeling of geometries, solving geometries using specified conditions, and visualization of the results.

The geometry is made up of two basic parts: the blocks and the mesh. The blocks form the outline of the structure being modeled. Taking advantage of the axial symmetry of the resonator, a 2-D model was generated using cylindrical coordinates. The geometry is constructed as a "slab", and when transferred to the solver, this slab is read in as a wedge. Figure 2 shows the slab of the resonator as it is portrayed in the CFX modeling program.

Creating a mesh is the second step in developing the model geometry. The average mesh density for this geometry was 10 units of mesh per 1 inch of surface. (A CFX mesh density of .1) A biased mesh was used at the walls of the resonator. The mesh for this problem is shown in Fig's 3 and 4. In Fig. 3, the mesh in one bulb/end of tapered region is shown. In the transition region between the channel and the bulb, the mesh was refined at the wall. In Fig. 4, the mesh in the connecting channel is shown. The grid density was increased near the wall to aid in resolving the boundary layer. Compressible, turbulent flow with a k-ε model is used. When this model is used within CFX4.2, the boundary layer between the center of the cell closest to the wall and the wall is resolved using the law of the wall approximation. For the cells next to the wall, the y^+ values were all less than 150. A total of 8160 mesh elements were used.

The problem is solved transiently over a period of approximately 0.062 seconds. A value of 2.22×10^{-5} seconds is used for the first 100 timesteps and 1.11×10^{-4} is used for the remaining timesteps. The working fluid is argon gas. Initially, the gas was held in the right-hand bulb of the model at a pressure of 862 kPa and the left-hand bulb at 517 kPa, both at a temperature of 25°C. These values were chosen to match the laboratory test case.

RESULTS AND DISCUSSION

Using the CFD simulation, the flow characteristics can be observed for the fluid as it passes through the taper into the bulb. Figure 5 shows how the fluid detaches from the wall and creates a plume within the bulb. It is interesting to note that the fluid detaches from the wall while still within the gentle 7° taper. The cause for this early detachment may be the combination of both spatial and temporal adverse pressure gradients, *i.e.* the fluid is decelerating due to the diffuser and due to the oscillating nature of the flow. The effects of temporal adverse pressure gradients is a subject of future study.

The length of the solution allowed for just under one and a half oscillation cycles to be modeled. Figure 6 shows a plot of pressure versus time for both the experimental and simulated resonators. Pressure for this plot was measured in the bulb on the left side of the resonator. The comparison between the measured and simulated frequency is good. The difference may be attributable to construction tolerances in the experimental resonator.

The initial amplitude of the simulated pressure oscillation (at about 0.03 sec) is in fairly good agreement with the experiment. The discrepancy in initial amplitude may be due to the finite time required for the valve to open in the experiment. To compare the dissipation in the experiment and calculation, we calculate the oscillation energy lost per half cycle in two different ways. The energy stored in the oscillation E is proportional to the square of the amplitude of the oscillation A, *i.e.* $E=\alpha A^2$ where α is a constant of proportionality that depends on the resonator geometry. Therefore, the energy decrement in a half cycle can be estimated as $\Delta E_1 \sim 2\alpha \langle A \rangle \Delta A$ where $\langle .. \rangle$ represents the average of the amplitude at the beginning and end of the half cycle. At the high velocities in the experiment, we expect the dissipative pressure drop to be proportional to v^2 where v is the velocity in of the flow in the connecting pipe. Therefore, the rate of energy loss will be proportional to v^3, *i.e.* $dE/dt=\beta A^3$ where β is a constant given by the minor loss coefficients of the tapered sections and abrupt expansions as well as the friction factor in the connecting and tapered sections. The energy decrement over the half cycle can now be estimated by $\Delta E_2 \sim \beta \langle A \rangle^3 T/2$ where T is the period of the oscillation. Setting $\Delta E_1=\Delta E_2$, we find $\beta T/4\alpha=\Delta A/\langle A \rangle^2$. Using the half cycle between 0.03 and 0.05 seconds, we find $\Delta A/\langle A \rangle^2=0.0054$ and 0.0053 in the simulation and experiment, respectively. Since α only depends on resonator geometry and the simulation correctly predicts T, the simulation is also correctly predicting β, the overall dissipation coefficient.

The velocity profiles were sampled from the simulation in the center of the connecting pipe. Velocity profiles versus radial distance from the wall for one full period of oscillation are shown in Fig. 7. These profiles were sampled every $\pi/4$ periods of the oscillation starting with the first zero-crossing location in Fig. 6. The peak Reynolds number for this flow is on the order of 10^6. For a given profile, each data point represents the velocity at the center of the computational cell. The software uses a law-of-the-wall approximation for the velocity between the wall and the nearest cell center. These profiles have the correct qualitative behavior. At lower Reynolds number, the profile (not shown) should display characteristic peaks about 1 or 2 viscous penetration depths (about 0.4 mm) away from the wall [2]. At the high Reynolds numbers in Fig. 7, these peaks are replaced by a velocity that decreases with a power-law behavior from the center of the pipe to the wall. This is consistent with past experimental studies of oscillating pipe flow [2].

CONCLUSION

CFD promises to be a useful tool in the analysis of transient, oscillating flow phenomenon. The agreement between this simulation and the matching experiment is encouraging. Using the results of the CFX model, both experimental correlation and new discoveries have been made. CFX was able to qualitatively depict the oscillating flow characteristics and provide insight into the details of the resonator's operation.

ACKNOWLEDGMENTS

Shiv Shivaraman of AEA Technology provided support in the development and solution of the computational model. Thad Knight of Los Alamos National Laboratory made the properties of argon available by providing a PCP fluid database. David Gardner designed the experimental resonator and valve and provided Fig. 1.

REFERENCES

1. Backhaus, S. and Swift, G.W., 1999, "A Thermoacoustic Stirling Heat Engine," *Nature*, Vol. 399, pp. 335-338.
2. Ohmi, M. and Iguchi, M., 1982, "Critical Reynolds Number in an Oscillating Pipe Flow," *Bulletin of the JSME*, Vol. 25, No. 200.

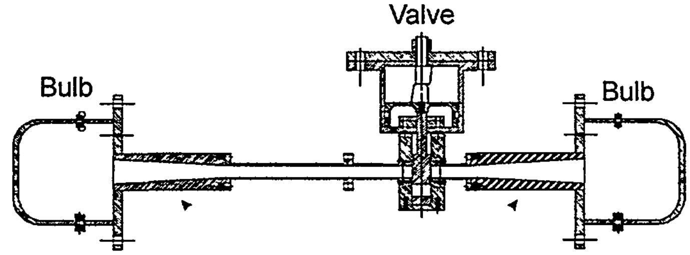

Fig. 1. Acoustic Resonator.

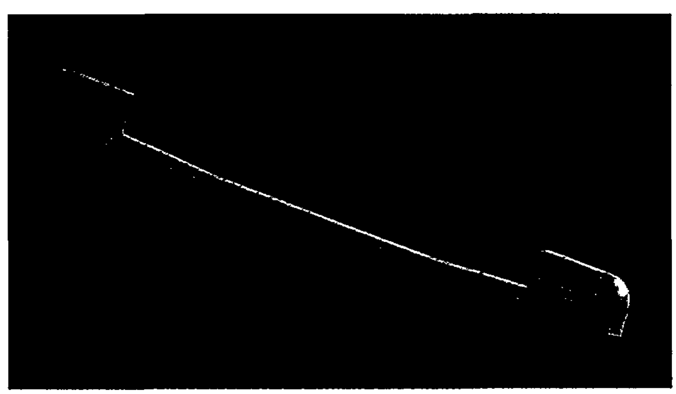

Fig. 2. Block Structure of 2-D, CFD Model.

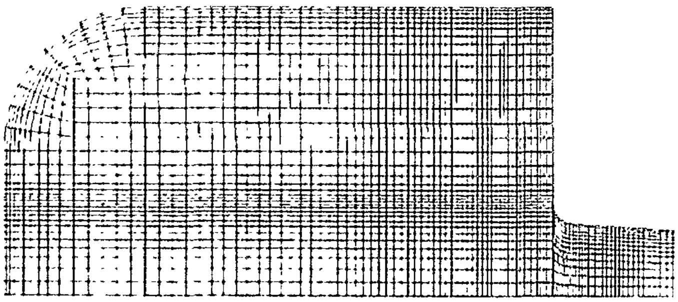

Fig. 3. 2-D Mesh In Bulb/Tapered Region.

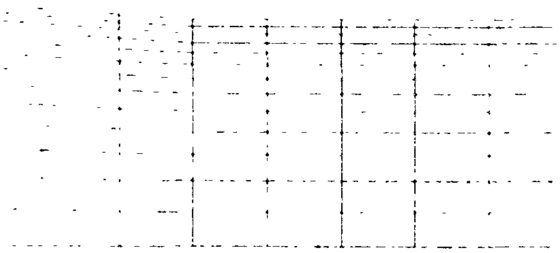

Fig. 4. 2-D Mesh In Channel Region

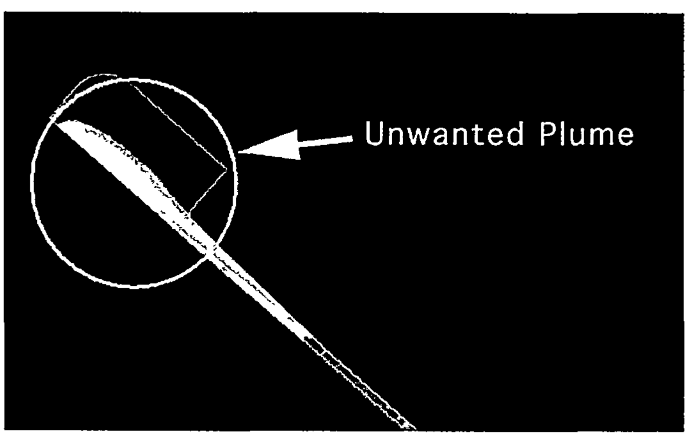

Fig. 5. Plume In Bulb. Blue represents high velocities. Red represents low velocities.

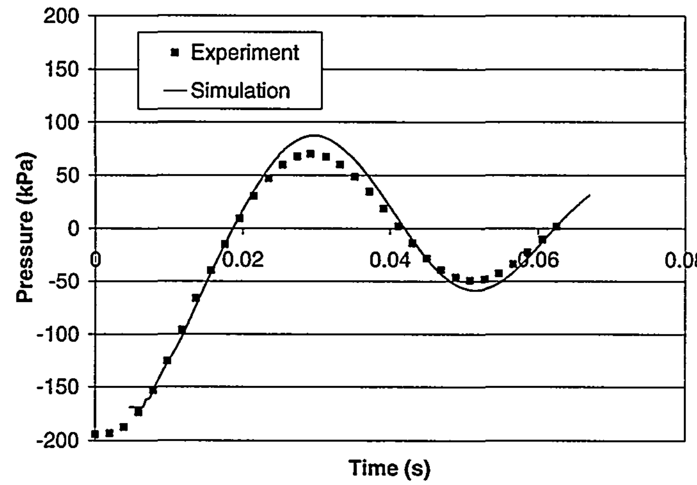

Fig. 6. Pressure Oscillations. The calculated pressure curve (simulation) has been shifted to the right to force the first zero crossing to coincide with the experimental data. This time delay is of the same order as the time required for the valve to open in the experiment. This may also be responsible for the lower oscillation amplitude in the experimental data.

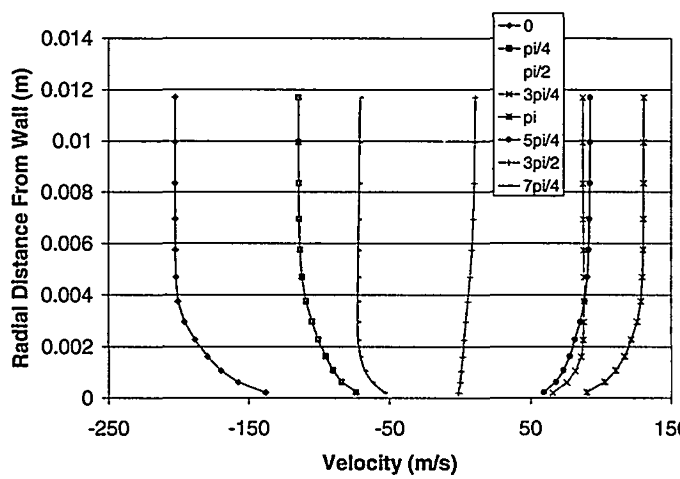

Fig. 7. Velocity Profiles.